

Characterization of Magnesium Substituted Nickel Nano Ferrites Synthesized By Citrate-Gel Auto Combustion Method

Abdul Gaffoor and D. Ravinder*

Department of Physics Osmania University Hyderabad-500007

ABSTRACT

Ni-Mg nano-ferrites, having the chemical formula $Ni_{1-x}Mg_xFe_2O_4$ (where $x = 0.0, 0.2, 0.4, 0.6, 0.8, 1.0$), were synthesized by the Citrate- gel auto combustion method. Synthesized powders were sintered at $500^\circ C$ for 4 hours in an air and were characterized by XRD, SEM and EDS. XRD analysis showed cubic spinel structure of the ferrites and the crystallite sizes (D) were found in the range of 16 nm - 36 nm. The values of lattice parameter (a) increases with the increase of Mg content obeying Vegard's law. The x-ray density of the samples decrease monotonically with increasing Mg content. Scanning Electron Microscopic (SEM) studies revealed nano crystalline nature of the samples. An elemental composition of the samples was studied by Energy Dispersive Spectroscopy (EDS). The observed results can be explained on the basis of composition and crystal size.

Keywords: Ni-Mg Nano-Ferrites; Citrate-Gel Auto Combustion; X-Ray Diffraction; SEM; EDS

I. INTRODUCTION

Ferrites form a very good class of electrical materials because of their high resistivity and low loss behaviour, and hence have vast technological applications over a wide range of frequencies. Ferrites are preferred in the field of electronics and telecommunication industry because of their novel electrical properties which makes them useful in radiofrequency circuits, high quality filters, rod antennas, transformer cores, read/write heads for high digital tapes and other devices. Hence it is important to study their dielectric behaviour at different frequencies. The dielectric properties of ferrites are dependent on several factors, such as method of preparation, heat treatment, sintering conditions, chemical composition, cation distribution and crystallite size [1].

Ferrites, a distinct class of magnetic materials known as ferromagnetic have spinel structure. They consist of spontaneously magnetized domains and show the phenomena of magnetic saturation and hysteresis. Spinel ferrites possess properties of both magnetic materials and insulators and are important in many technological applications. The interesting physical and magnetic properties of spinel ferrites arise from the ability of these compounds to distribute the cations among the available tetrahedral (A) and octahedral (B) sites [2]. Spinel ferrites have gained lot of attention because of their remarkably high electrical and magnetic flux induction. They are considered as good dielectric and are found in many technological applications. Increased application of ferrites has led to the development of many chemical methods which

includes hydrothermal, co-precipitation and sol-gel for the preparation of stoichiometric and chemically pure spinel ferrites [3].

Nickel ferrites are known for high power handling capability at microwave frequencies due to their high curie temperature which makes other magnetic properties of this series relatively independent of temperature [4]. Nickel and Magnesium ferrite is extensively used in a number of electronic devices due to their high permeability at high frequency, remarkable high electrical resistivity, mechanical hardness, chemical stability and reasonable cost [5]. $NiFe_2O_4$ is a well known inverse spinel with Ni^{2+} at octahedral [B-site] and Fe^{3+} ions distributed equally in tetrahedral (A-site) and octahedral sites [B-site] [6]. Magnesium ferrite ($MgFe_2O_4$) is one of the most important ferrites. It has a cubic structure of normal spinel-type and is a soft magnetic n-type semiconducting material, which finds a number of applications in heterogeneous catalysis, adsorption, sensors, and in magnetic technologies [7]. Recently, nanostructures of magnetic materials have received more and more attention due to their novel material properties that are significantly different from those of their bulk counterparts [8-12].

In this study, samples with the formula $Ni_{1-x}Mg_xFe_2O_4$ ($x=0.0, 0.2, 0.4, 0.6, 0.8$ and 1.0) were synthesized via the Citrate gel Auto-Combustion method. The energy to form the ferrite nanocrystallites is provided by oxidation-reduction process of thermal precursor and fuel in the Citrate - Gel auto-combustion process [13].

II. Experimental

2.1. Synthesis

A series of Magnesium substituted Nickel nano ferrites having the chemical formula $Ni_{1-x}Mg_xFe_2O_4$ (where $x = 0.0, 0.2, 0.4, 0.6, 0.8$ and 1.0) were prepared by Citrate Gel Auto-combustion method. The starting materials were Nickel Nitrate ($Ni(NO_3)_2 \cdot 6H_2O$), Ferric Nitrate ($Fe(NO_3)_3 \cdot 9H_2O$), Magnesium Nitrate ($Mg(NO_3)_2 \cdot 9H_2O$), Citric acid ($C_6H_8O_7 \cdot H_2O$) and Ammonia (NH_3) all of 99% pure AR grade. Metal nitrates were employed in this process as they have a dual role of being a soluble cation sources and the oxidant [14]. Calculated quantities of metal nitrates were dissolved together in a minimum amount of distilled water to get clear solution. An aqueous solution of Citric Acid was then added to the metal nitrate solution. Citric acid was used with 2 important roles: the fuel for the combustion reaction and as a chelating agent to form complexes with metal ions, preventing the precipitation of hydroxylated compounds [15]. The molar ratio of Citric acid to the total moles of nitrate ions was adjusted to 1:3. The mixture was stirred to obtain a homogeneous solution and then was slowly

heated to $80^\circ C$ at a rate of $5^\circ C/minute$ using a hot plate magnetic stirrer. P^H of the solution was adjusted to 7 by adding Ammonia (NH_3) solution. A Sol is formed. The resulting solution was evaporated to dryness by heating at about $150^\circ C$ on a hot plate with continuous stirring. As a result the viscosity rose due to cross linking of carboxylato-metal complexes into a three dimensional structure (pi-erre *et al.*, 1990; Jang *et al.*, 1995, Narebder abd Messing, 1997) and get started to form a viscous gel (**Figure 1(a)**). When finally all water molecules were removed from the mixture by increasing the temperature to $200^\circ C$, the viscous gel began frothing. The gel gave a fast flameless auto combustion reaction with the evolution of large amounts of gases (**Figure 1(b)**). It started in the hottest zones (**Figure 1(c)**) of the beaker and propagated from the bottom to the top like the eruption of a Volcano (**Figure 1(d)**). The reaction was completed in a minute giving rise to dark grey voluminous product with a structure similar to Branched tree (**Figure 1(e)**). Finally the burnt powder was ground and was calcined in air at temperature $500^\circ C$ for four hours to obtain a spinel phase.

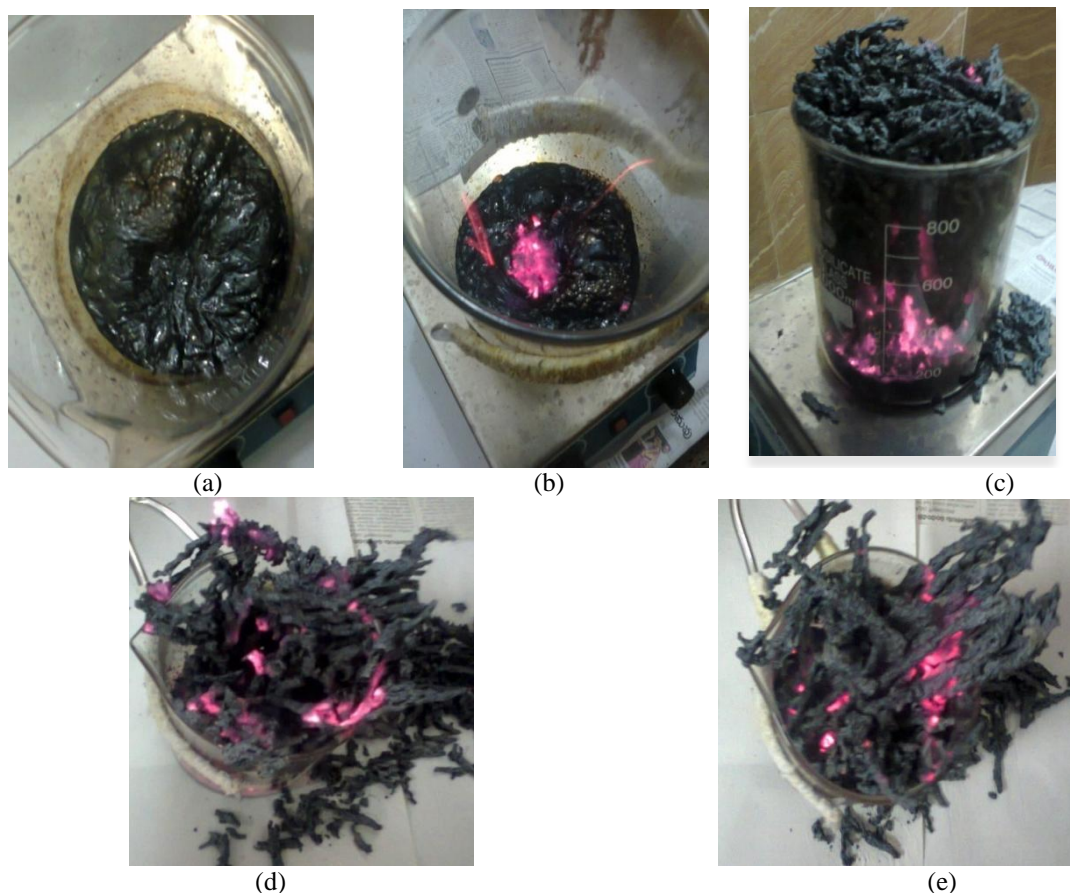


Figure 1.(a) Viscous gel formation; (b) Self ignition (c) Combustion of mixture;(d) propagation of combustion like Volcanic eruption; (e) Dark grey voluminous product with a structure Similar to a branched tree

2.2. Characterization

X-ray Diffraction with Cuka ($\lambda = 1.54 \text{ \AA}$) was used to study the single phase nature and nano-phase formation of the Ni-Mg ferrite system at room temperature by continuous scanning in the range of 10° to 90° degrees.

Micro structural analysis of the prepared samples was carried out by scanning Electron microscopy (SEM) and elemental compositional analysis for all samples was done by Energy Dispersive Spectroscopy (EDS).

III. Results and Discussions

3.1. XRD Analysis

The X-ray diffraction patterns of all the samples were shown in **Figure 2**. XRD patterns and the crystalline phases were identified by comparison with reference data from the ICSD card No. 22 -1086 for Magnesium ferrites ($\text{Mg Fe}_2\text{O}_4$). The XRD patterns of all the Magnesium substituted nickel ferrites showed a homogeneous single phased cubic spinel belonging to the space group Fd3m (confirmed by ICSD Ref 22-1086). All the Bragg reflections have been indexed, which confirmed the formation of

a well defined single phase cubic spinel structure without any impurity peaks. All the peaks are allowed peaks. The strongest reflection has come from (311) plane that indicates spinel phase.

The diffraction peaks can be indexed to the planes of (2 2 0), (3 1 1), (2,0 0), (5 1 1) and (4 4 0). The observed broadening of diffraction peaks indicates the nano-crystallinity of the samples. The particle size of the synthesized ferrite samples was estimated from X-ray peak broadening of diffraction peaks using Scherrer formula [16]. The values of the particle size, lattice constant and X-ray density as deduced from the X-ray data are given in **Table 1**

$$t = \frac{0.91\lambda}{\beta \cos \theta}$$

where λ = Wavelength of X-ray, β = Full width and Half Maxima in radians, θ = Bragg's angle at the peak position.

Lattice parameter "a" of individual composition was calculated by using the following formula and values were tabulated in **Table 1**.

$$d = \frac{a}{\sqrt{h^2+k^2+l^2}}$$

where a = lattice parameter, d = inter planar distance, hkl = miller indices.

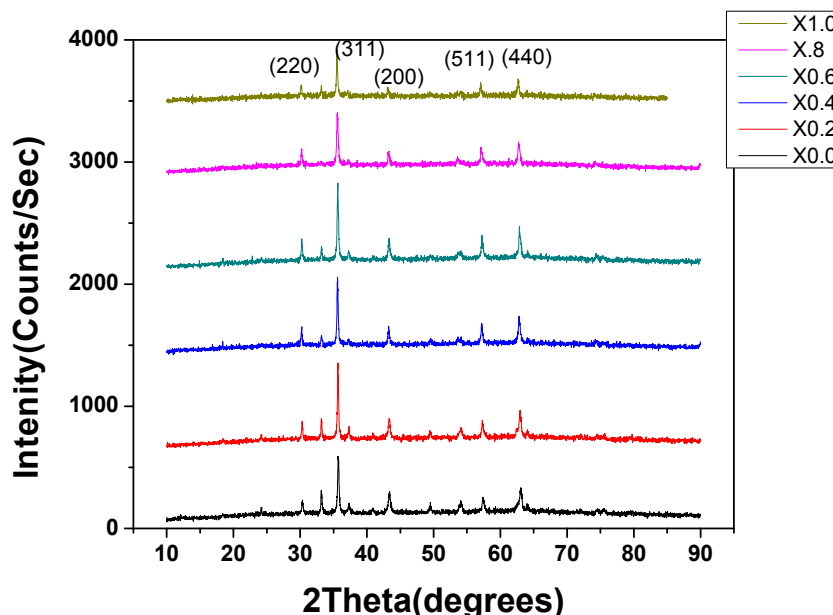


Figure 2. XRD of $\text{Ni}_{1-x}\text{Mg}_x\text{Fe}_2\text{O}_4$ (where $x = 0.0, 0.2, 0.4, 0.6, 0.8, 1.0$)

The variation of lattice parameter with Mg compositions was shown in **Figure 3**. The lattice parameter was found to increase linearly with increasing Mg concentration. This linear variation indicates that the Ni-Mg ferrite system obeys Vegard's law [17]. The lattice constant increases with

magnesium doping, which can be explained based on the relative ionic radius. The ionic radius (oct: 0.72 \AA) of Mg^{2+} ions is larger than the ionic radius (oct: 0.69 \AA) of Ni^{2+} ions. Replacement of smaller Ni^{2+} cations with larger Mg^{2+} cations causes an increase in lattice constant.

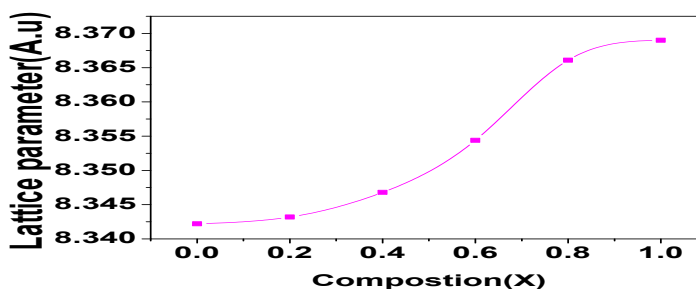


Figure 3 Variation of Lattice Parameter(a) with Composition(x) for Ni-Mg nano-ferrites

X-ray density (d_x) for different compositions was calculated using the formula [18] and calculated values were tabulated in Table 1.

$$d_x = \frac{ZM}{Na^3} \text{ gm/cc}$$

where Z = Number of molecules per unit cell (8), M = Molecular weight of the sample, N = Avagadro's Num-ber, a = lattice parameter.

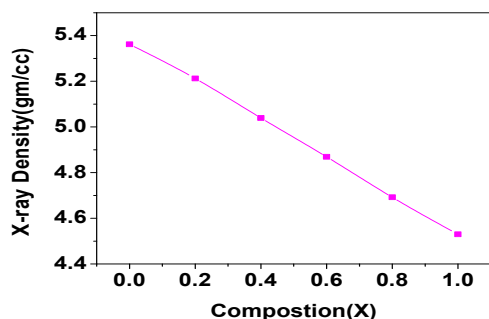


Figure 4 Variation of X-ray density with Composition(X) for Ni-Mg nano-ferrites

The X-ray density is expected to decrease with the Mg content because the lattice parameter increase with Mg content. Similar result has been observed by Pandit et al. in Mg-Mnferrites[19] and by M.A. Gabal, et al., in Ni-Mg Nanoferrites by egg white Precursor Method[20]. The decrease in X-ray density can be ascribed to the atomic weight and density of Mg^{2+} (24.31 and 1.74 gm/cm³), which are lower than those of Ni^{2+} (58.69 and 8.90 gm/cm³) and Fe^{3+} (55.85 and 7.86 gm/cm³) [21].

Volume of unit cell was calculated by using the formula

$V = a^3$ in A⁰ units where 'a' is lattice parameter. Volume of unit cell was found to increase with increase in Mg content, as it depends on lattice parameter which has increased with increase in Mg content.

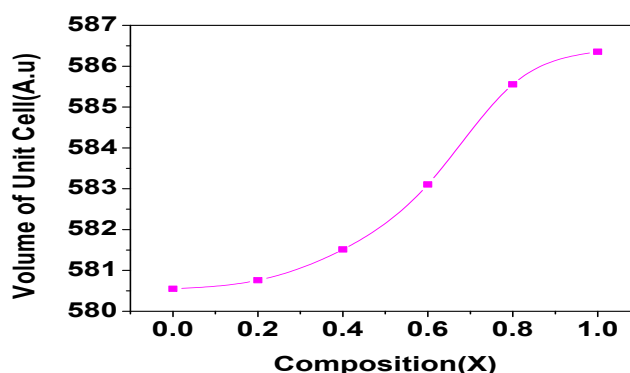


Figure 5 Variation of Volume of Unit cell with Composition(X)

The distance between magnetic ions (hopping length) in A site (tetrahedral) and B site (octahedral) were calculated using the relations

$$d_A = 0.25a\sqrt{3} \quad d_B = 0.25a\sqrt{2}$$

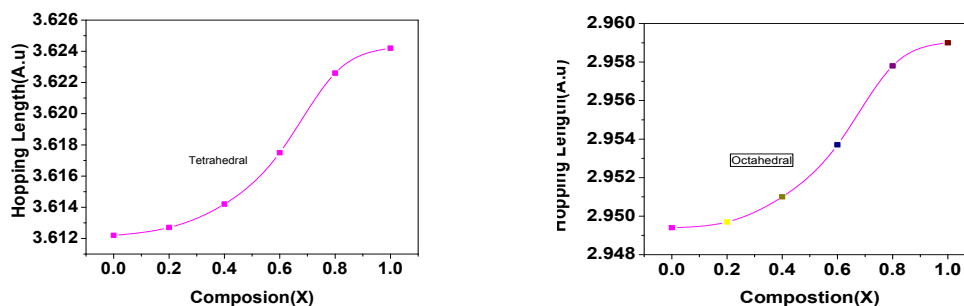


Figure 6 The distance between magnetic ions in both Octahedral and tetrahedral Sites as a function of Composition (X) for Ni-Mg nano-ferrites

The calculated values of the hopping length for Tetrahedral site (d_A) and octahedral (d_B) of different compositions were tabulated in **Table 1**. The relation between hopping length for Octahedral

and Tetrahedral sites as a function of Mg content(x) was shown in **Figure 6**. It is observed that the hopping length increases as the Mg content increases.

Table 1. Values of Crystallite size, Lattice parameter(a), unit cell volume, X-ray density and hopping length for A-Site(d_A) and B-Site(d_B) of Ni-Mg Nano ferrite with Composition(X=0.0,0.2,0.4,0.6,0.8,1.0)

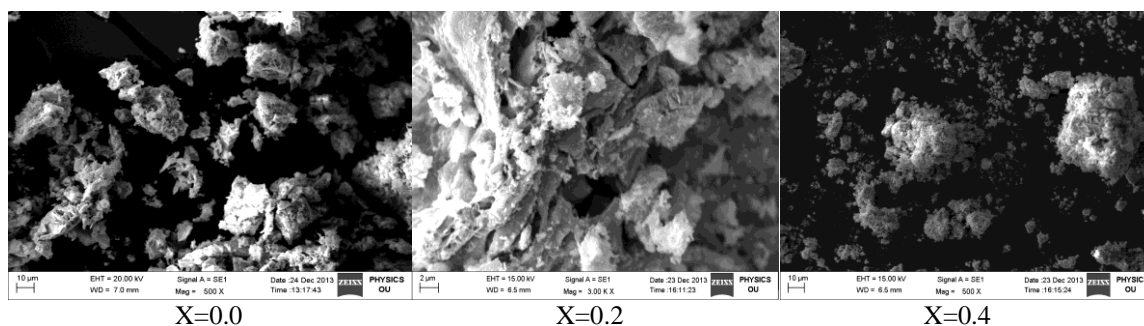
Sample	Particle size	Lattice parameter(A.u)	Unit cell volume(A.u)	X-Ray density(gm/cc)	A site d_A (A.u)	B Site d_B (A.u)
NiFe ₂ O ₄	23.57nm	8.3422	580.552	5.362	3.6122	2.9494
Ni _{0.8} Mg _{0.2} Fe ₂ O ₄	35.8 nm	8.3432	580.7616	5.212	3.6127	2.9497
Ni _{0.6} Mg _{0.4} Fe ₂ O ₄	30.7 nm	8.3468	581.513	5.039	3.6142	2.9510
Ni _{0.4} Mg _{0.6} Fe ₂ O ₄	29.6 nm	8.3544	583.103	4.869	3.6175	2.9537
Ni _{0.2} Mg _{0.8} Fe ₂ O ₄	34.0nm	8.3661	585.556	4.692	3.6226	2.9578
MgFe ₂ O ₄	16.5nm	8.369	586.355	4.530	3.6242	2.9590

3.2. Morphology by SEM

Morphology of the prepared samples by Citrate-gel method was studied using scanning electron microscope (SEM) where the secondary electron images were taken at different magnifications to study the morphology. The scanning electron microscopic images of all the synthesized samples were shown in **Figure 7**.

The images show that the particles have an almost homogeneous distribution, and some of them are in agglomerated form. It is evidenced by SEM

images that the aggregation of particles lies in nano-metric region. The particles were observed as uniform grains (in different SEM images) confirming the crystalline structure of Ni-Mg nano ferrites which were detected by XRD studies. The formation of Fe₂O₄ was chemically favoured by heating during the synthesis where as final reaction was completed during the sintering where the pores between the particles were removed combined with growth and strong bonds by agglomeration.



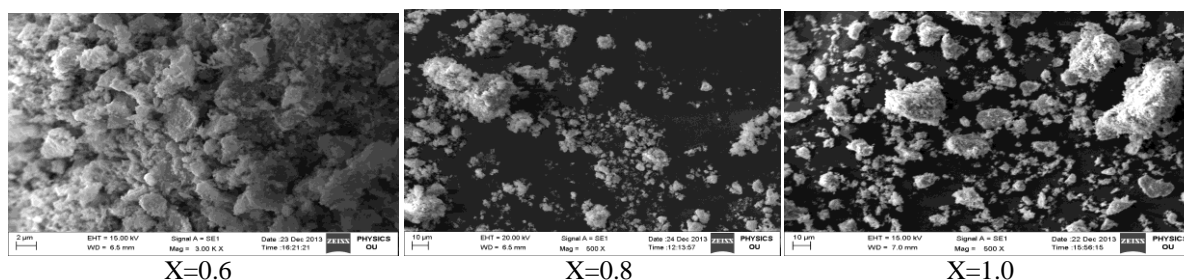


Figure 7 SEM images of $Ni_{1-x}Mg_xFe_2O_4$ Nano ferrites

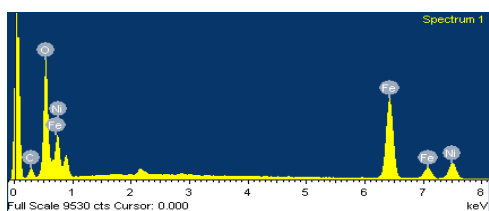
3.3. Elemental Analysis by EDS

The elemental analysis of all the Ni-Mg nano ferrite samples with different compositions was analysed by Energy Dispersive Spectrometer (EDS) and the elemental % and atomic % of different elements in the were shown in the **Table 2**. The EDS

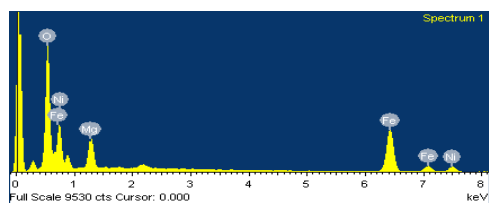
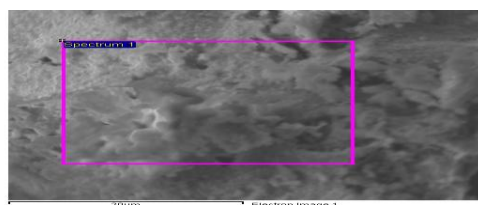
pattern for samples with $x = 0.0, 0.6$ and 1.0 were shown in **Figure 8** which indicates the elemental and atomic composition in the sample. The compounds show the presence of Ni, Mg, Fe and O without precipitating cations.

Table 2 Elements of each sample composition Ni-Mg Nano ferrites analysed by (% weight) obtained by EDS

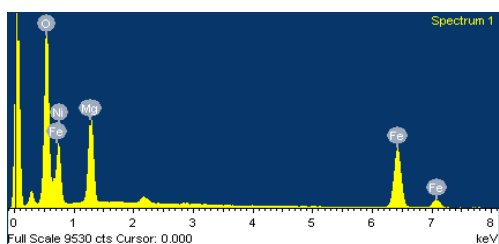
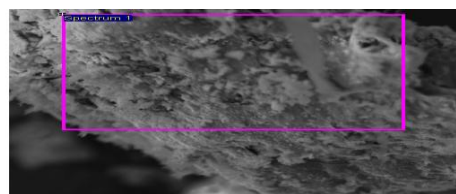
Element Ferrite composition	O		Ni		Mg		Fe	
	element %	Atomic %	element %	Atomic %	element%	Atomic%	Element %	Atomic %
NiFe₂O₄	29.93	61.88	18.12	9.50	-----	-----	51.92	28.62
Ni_{0.8}Mg_{0.2}Fe₂O₄	30.72	59.09	15.83	8.28	4.55	5.75	48.85	26.87
Ni_{0.6}Mg_{0.4}Fe₂O₄	37.56	67.20	15.32	7.47	1.78	2.10	45.33	23.23
Ni_{0.4}Mg_{0.6}Fe₂O₄	36.25	63.51	9.15	4.37	7.25	8.35	47.35	23.77
Ni_{0.2}Mg_{0.8}Fe₂O₄	29.36	55.78	5.80	3.00	8.39	10.50	56.45	30.72
MgFe₂O₄	38.37	62.91	-----	-----	13.37	14.42	48.38	22.72



(X=0.0) NiFe₂O₄ Nano ferrite



(X=0.6) Ni_{0.4}Mg_{0.6}Fe₂O₄ Nano ferrite



(X=1.0) MgFe₂O₄ Nano Ferrite

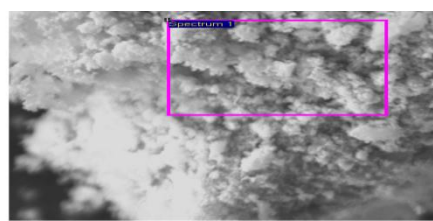


Figure 7 EDS graph of $Ni_{1-x}Mg_xFe_2O_4$ Nano ferrites with composition (X=0.0,0.6,1.0)

IV. Conclusions

- Citrate Gel auto combustion technique is a convenient way for obtaining a homogeneous nano sized mixed Ni-Mg ferrites.
- The process involves no impurity pickup and material loss. It is a very simple and economical method where no specific heating or cooling rate is required. It is a low temperature processing technique and requires shorter sintering duration.
- X-ray diffraction pattern confirms the formation of cubic spinel structure in single phase without any impurity peak. It is in good agreement with the standard data from ICSD
- The crystallite size of the various Ni-Mg ferrites was in the range of 16-36nm.
- The lattice parameter is increased with the increase of Mg substitution in Ni-Mg ferrites which indicates that the mixed Ni-Mg ferrite system obeys Vegard's law.
- SEM micrographs of various compositions indicate the morphology of the particles is similar. They reveal largely agglomerated, well defined nano particles of the sample powder with inhomogeneous broader grain size distribution.
- EDS data gives the elemental% and atomic % in the mixed Ni-Mg nanoferrites and it shows the presence of Ni, Mg, Fe and O without precipitating cations.

V. Acknowledgment

The authors are very thankful to Prof.K.Venugopal Reddy, Head, Department of Physics, University College of Science, Osmania University, Hyderabad for his support and encouragement to carry out this research work.

References

- [1] M. Abdullah Dar, Khalid MujasamBattoo, VivekVerma, W.A. Siddiqui, R.K., "Synthesis and characterization of nano-sized pure and Al-doped lithium ferrite having high value of dielectric constant" Journal of Alloys and Compounds, 493,pp 553-560,2010.
- [2] K.H.Maria, S.Choudhary,M.A.Hakim , "Complex Permeability and Transport Properties of Zn Substituted Cu ferrites",Journal of Bangladesh Academy of Sciences,Vol.34, No1,pp1-8,2010.
- [3] M.H.Khedr, , "Effect of firing temperature and compacting pressure on the magnetic and electrical properties of nickel ferrite",Journal of physicochemical problems of mineral processing, Vol 38,pp 311-320,2004.
- [4] N.S. Bhattacharyya, G.P.Srivatava,On the instability threshold of cobalt substituted Ni-Al ferrite at high-microwave- power levels, J .Mag & Mag. Mat.262,pp 212,2003.
- [5] Ishino K &NarumiyaY,Ceram Bull 66(1987)1469.
- [6] Zhou Z H ,Xue J M,Wang J, Chan H S O,Yu T &Shen Z X,J Appl Phys,91 (2002) 6015.
- [7] R.J. Willey, P. Noirclerc, G. Busca, Chem. Eng. Commun. 123, 1 (1993). doi:10.1080/00986449308936161
- [8] S. Choi, M.H. Chung, Semin. Integr. Med. 1, 53 (2003) .
- [9] Z. Lai, G. Xu, Y. Zheng, Nanoscale Res. Lett. 2, 40 (2007). doi:10.1007/s11671-006-9027-3
- [10] S.A. Corr, Y.P. Rakovich, Y.K. Gun'ko, Nanoscale Res. Lett. 3,87 (2008). doi:10.1007/s11671-008-9122-8
- [11] S. Wang, Y. Zhou, W. Guan, B. Ding, Nanoscale Res. Lett. 3,289 (2008). doi:10.1007/s11671-008-9151-3
- [12] W. Wu, Q. He, C. Jiang, Nanoscale Res. Lett. 3, 397 (2008).doi:10.1007/s11671-008-9174-9.
- [13] K. H. Wu, T. H. Ting, M. C. Lia and W. D. Ho: J. Magn. Magn. Mater, 2006, vol. 298, pp. 25-32.
- [14] H. Chyi-Ching, W. Tsung-Yung, W. Jun, T. Jih-Sheng: Mater. Sci. Eng. B, 2004, vol. 111, pp. 49-56.
- [15] J Livage, C. Sanchez, M.Henry and S. Doeuff: Solid State Ionics, 1989, vol. 32/33, pp. 633-638.
- [16] B. D. Cullity, "Elements of XR-Diffraction," Addison Weseley Publishing, Reading, 1959, p. 132.
- [17] L. Vegard, "The Constitution of Mixed Crystals and the Space Occupied by Atoms," Zeitsch rift fir Physics, Vol. 5, No. 17, 1921, pp.17-23.
- [18] R. C. kumbale, P. A. sheikh, S. S. Kamble and Y. D. kolekar, "Effect of Cobalt Substitution on Structural Ma-gnetic and Electric Properties of Nickel Ferrite," Journalof Alloys and Compounds, Vol. 478, No. 1-2, 2009, pp.599-603. doi:10.1016/j.jmmm.2005.03.007
- [19] A.A Pandit, A.R. Shitre, D. R. shengule, K.M. Jadhav, J. of Mater.Sci.40 [2](2005) 423-428.
- [20] M.A. Gabal, et al., Journal of Magnetism and Magnetic Materials (2014), http://dx.doi.org/10.1016/j.jmmm.2014.03.007i
- [21] C. Kittel, introduction to solid state physics, seventh Ed., Wiley, Singapore(1996).